

Structural relaxation and relative stability of nanodiamond morphologies

A.S. Barnard, S.P. Russo*, I.K. Snook

Department of Applied Physics, Royal Melbourne Institute of Technology, GPO Box 2476V, Melbourne 3001, Victoria, Australia

Abstract

Presented here are the results of ab initio Density Functional Theory (DFT) relaxations performed on nanocrystalline diamond structures of cubic {100}, octahedral {111} and cuboctahedral morphologies, up to approximately 1 nm in diameter. Results show that in this size range, the crystal morphology plays an important role in the structural stability of the crystals, in the absence of external fields. While the surfaces of the cubic crystals exhibited reconstruction and relaxations comparable to that of bulk diamond, the surfaces of the octahedral and cuboctahedral crystals showed the transition from sp^3 to sp^2 bonding. Our results demonstrate the inward transition of nanodiamond clusters into carbon onion-like structures, with preferential exfoliation of the (111) surfaces, in agreement with recent experimental observations. The results of this study will provide a better understanding of the effects of nanodiamond morphology on the stability of diamondoid nanostructures and nanodevices.

© 2003 Elsevier B.V. All rights reserved.

Keywords: Nanodiamond morphologies; Density functional theory (DFT); Crystal morphology

1. Introduction

With the advent of nanotechnology related research in recent years, a great deal of interest has been generated in the study of nanocrystalline stability, including the relative stability of graphene and nanodiamond clusters [1–3]. The transformation of nanodiamonds of approximately 2–5 nm into carbon-onions has been observed experimentally, upon annealing at approximately 1200–1800 K, by a number of research groups [4–6] and modelled theoretically using semi-empirical [5,7–10] and ab initio methods [11,12]. It has been reported not only that the transition temperature is particle size dependent, but that the change occurs preferentially on the diamond (111) surfaces, over other lower index surfaces. Similarly, the transition of carbon-onions to nanocrystalline diamond under electron irradiation has been observed experimentally [13–17] and modelled theoretically [18] by means of atomic-scale computer simulations.

Presented here is a density functional theory (DFT) study of the energetics and relative stability (or metastability) at 0 K, of selected nanocrystalline diamond structures using the Vienna ab initio simulation package

(VASP) [19,20]. We used ultra soft, gradient corrected Vanderbilt-type pseudopotentials [21] as supplied by Kresse and Hafner [22] and the valence orbitals are expanded in a plane-wave basis up to a kinetic energy cutoff of 290 eV. These have been extensively tested for carbon and have been shown to give results in excellent agreement with all-electron ab initio methods [22,23] and good agreement with experiment [24].

The crystal relaxations were performed in the framework of DFT within the generalized-gradient approximation (GGA), with the exchange-correlation functional of Perdew and Wang [25], using an efficient matrix-diagonalization routine based on a sequential band-by-band residual minimization method (RMM) of single-electron energies [26,27], with direct inversion in the iterative subspace to minimize the electronic free energy. This technique has been shown to give results for bulk diamond in excellent agreement with experiment and has been successfully used previously in the study of bulk [28] and nanocrystalline diamond [11,12]. Both the ionic positions and symmetry were relaxed. Each ionic step consists of a minimum of three electronic steps, followed by calculation of the Hellmann–Feynman forces. Thus, both the symmetry and the lattice parameter of the nanocrystals were free to alter, resulting in expansions or contractions of the entire structures. The relaxations were performed for a minimum of 20

*Corresponding author. Tel.: +613-9925-2600; fax: +613-9925-5290.

E-mail address: salvy.russo@rmit.edu.au (S.P. Russo).

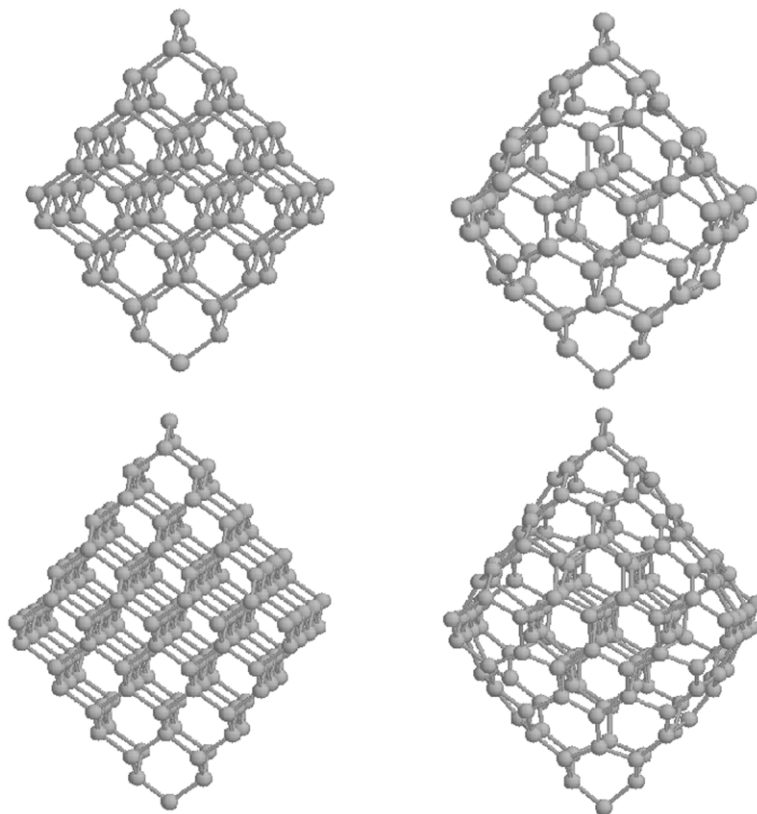


Fig. 1. C_{84} (top) and C_{165} (bottom) octahedral nanodiamond crystals before (left) and after (right) the relaxation process, viewed from the [100] direction.

ionic steps. While, this implies the minimum may only be local and not global, it is considered to be highly likely that such metastable structures may be formed during formation of nanocrystalline diamond, in the highly non-equilibrium synthesis environment. For this reason, all the crystals here are dehydrogenated and have not been annealed.

2. Relaxation of dehydrogenated nanodiamonds

The most significant result of these *ab initio* nanodiamond relaxations is a phase transition from the sp^3 bonding structure of diamond to the sp^2 bonding structure of graphite and fullerenes. Three octahedral nanodiamonds were investigated of the type used in the studies by Ree and Winter et al. [7,8]. These are the C_{35} , C_{84} and C_{165} octahedral structures, terminated by the C(111) (1×1) surface structure. Each crystal was surrounded by sufficient vacuum space and the structure optimized. The initial and final relaxed C_{84} and C_{165} crystals are given in Fig. 1. In the case of the C_{35} crystal, which is not shown here, an adoption of a more rounded appearance was observed.

The next largest octahedral nanodiamond, with 84 atoms was also found to adopt a rounded appearance. In this case, however, the 76 surface atoms appeared to

separate from the 8 atom inner core forming a carbon-onion like structure. The resulting outer carbon shell contained entirely sp^2 bonded atoms, with bond lengths of approximately 1.45 Å. This is significantly shorter than the C–C bond in bulk diamond, of 1.54 Å. The inner core was also found to contract, with the C–C bond lengths shortening to approximately 1.41 Å. The shell-core separation distance was found to be approximately 2.25 Å (see Fig. 1). The relaxation of the C_{165} atom octahedral carbon nanocrystal showed the same transition in which the 130 surface atoms separate from the 35 atom core cluster, forming a carbon-onion. Again, the bond length of the outer shell was shorter than the C–C bond in bulk diamond and the shell-core separation distance was found to be approximately 2.25 Å. The new ‘surface’ of the C_{35} core also exhibited a decrease in the C–C bond lengths (to approximately 1.41 Å), although the bonds connecting this ‘surface’ to the central atom were longer than the C–C bond in bulk diamond at approximately 1.60 Å. This process has been coined ‘buckification’ and is shown in Fig. 1.

Three structures were generated with cuboctahedral morphology; a C_{29} , a C_{142} and a C_{323} nanodiamond. This morphology is similar to that of a truncated octahedron, but with a surface area comprising 40%

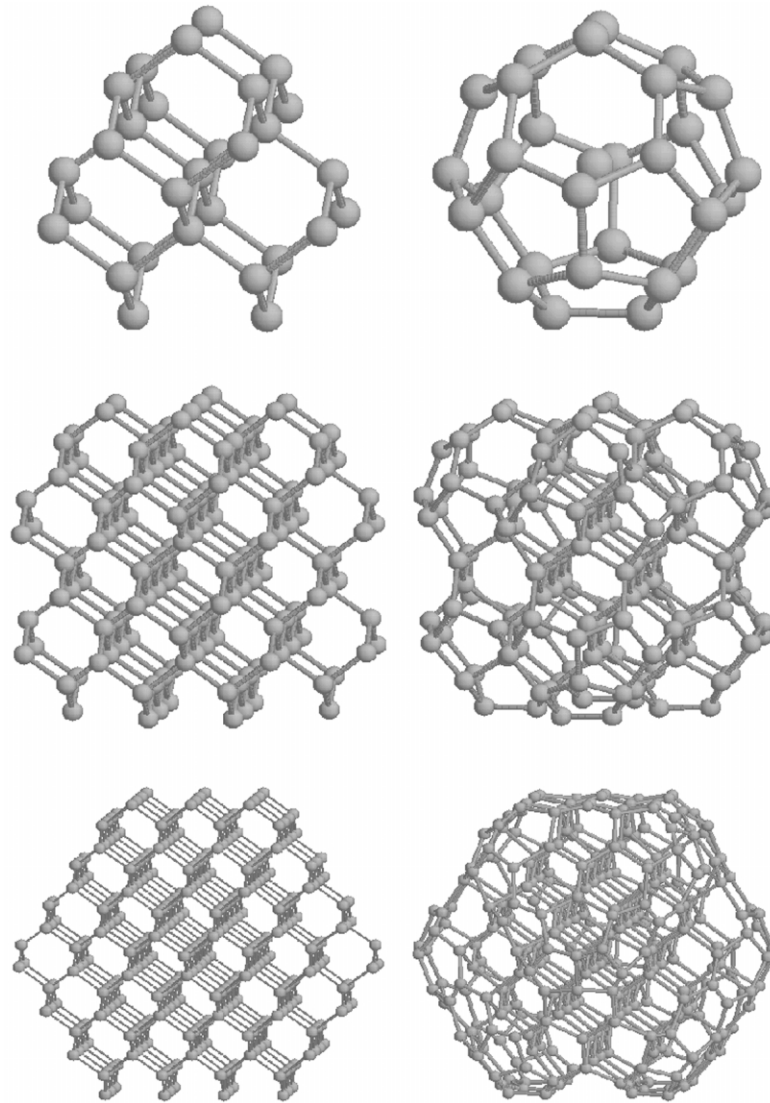


Fig. 2. C_{29} (top), C_{142} (centre) and C_{323} (bottom) cuboctahedral nanodiamond crystals before (left) and after (right) the relaxation process, viewed from the [100] direction.

{111} and 60% {100}. The results of the relaxation of C_{29} nanodiamond show the transformation of the nanocrystal into the C_{28} fullerene, with an endohedral carbon atom: C– C_{28} (see Fig. 2). The second cuboctahedron with 142 atoms also exhibited a transition from sp^3 to sp^2 bonding on the surface, but in this case the change only occurred on the (111) surface. The (100) surfaces initially reconstructed (thereby increasing the (111) surface area), followed by a re-orientation of the surface dimers to form the curved graphite-like (111) cages (see Fig. 2). This effect was, however, less pronounced in the C_{323} structure.

Finally, three cubic {100} structures were produced with 28, 54 and 259 atoms, respectively, and the relaxation performed. An important result in the comparison of the relative stability of various morphologies is that while the cuboctahedron with 29 atoms transformed into

a C– C_{28} endo-fullerene, the cubic nanodiamond structure with exactly 28 atoms becomes a metastable amorphous structure and not a fullerene (see Fig. 3). To ensure that this result is not an artifact of the length of the simulation (the number of ionic steps) the relaxation of the 28 atom cubic nanodiamond was allowed to proceed for over 120 ionic steps. The resulting cluster showed a slightly more amorphous structure but did *not* become a fullerene. This unusual result is under further investigation, as the VASP relaxation technique used here successfully predicts the C_{28} fullerene as the minimum energy structure. Preliminary analysis indicates that the lack of (111) surfaces may influence the onset of graphitization, and thus the transformation into fullerene-like structures.

The two larger cubic nanodiamonds were found to have surface reconstructions and relaxations comparable

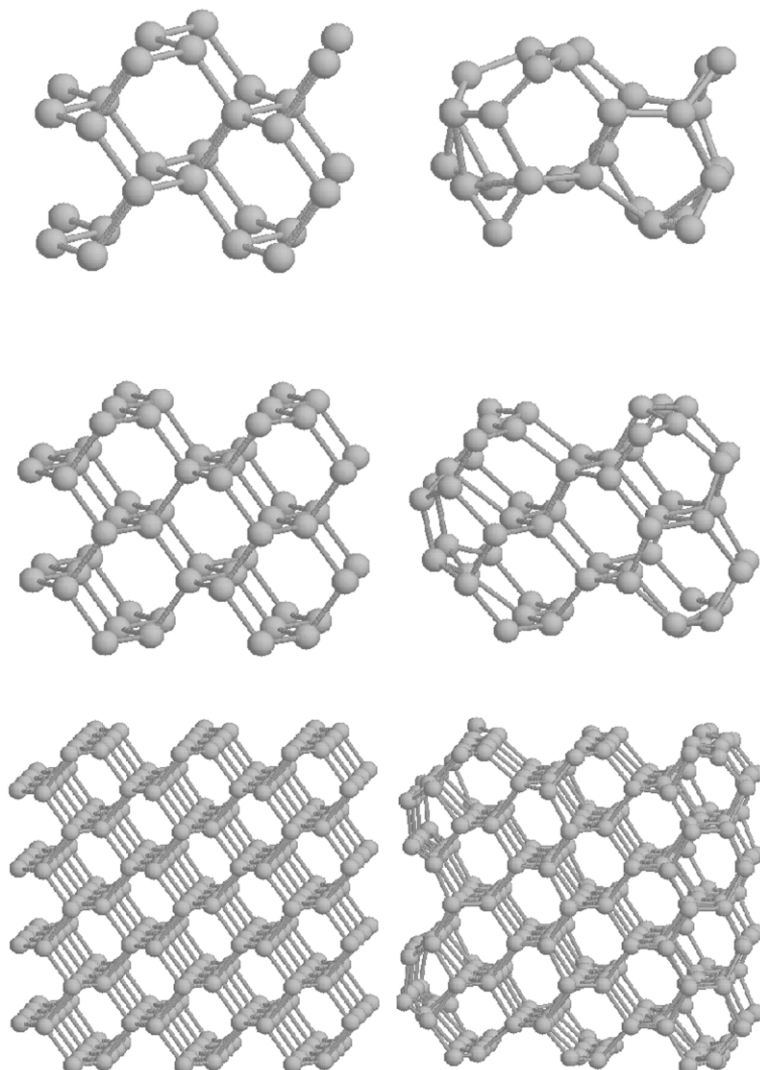


Fig. 3. C_{28} (top), C_{54} (centre) and C_{259} (bottom) cubic nanodiamond crystals before (top) and after (bottom) the relaxation process, viewed from the [100] direction.

to bulk diamond (see Fig. 3). A slight ‘shearing’ of the lattice was, however, observed in the case of the C_{54} crystal. The average (2×1) surface dimer lengths and the relaxation layer depths for the largest 259 atom cubic nanodiamond are given in Table 1, compared with

the DFT results of Furthmüller et al., using the ab initio molecular dynamics package VAMP [23], the semi-empirical density functional and experimental STM results for bulk diamond of Frauenheim et al. [29] and the ab initio LDA results of Yang et al. [30].

Table 1

Average relaxation and reconstruction properties of the dehydrogenated 259 atom cubic nanodiamond crystal, compared to the results of others for bulk diamond $C(100)(2 \times 1)$

	This study (DFT GGA)	VAMP DFT ^a	Semi-empirical ^b	DFT LDA ^c
d_{11} (Å)	1.44 ± 0.06	1.37	1.41	1.40
d_{12} (Å)	1.49 ± 0.08	1.50	1.50	1.52
Z_{12} (Å)	0.59 ± 0.07	0.67	1.1 ^d	–
Z_{23} (Å)	0.8 ± 0.17	0.79	–	–

^a Ref. [23].

^b Ref. [29].

^c Ref. [30].

^d Experimental STM from Ref. [29].

Table 2

Comparison of point groups before- (initial) and after (relaxed) the crystal relaxation for the octahedral and cuboctahedral nanodiamond structures. The point group and the error are suggested to be indicative of crystalline stability

Nanodiamond	Initial PG	Initial error	Relaxed PG	Relaxed error
C ₂₉	T _d	0.0000	C _{3v}	0.0000
C ₃₅	T _d	0.0000	T _d	0.0662
C ₈₄	T _d	0.0000	C _{3v}	0.0002
C ₁₄₂	T _d	0.0000	T _d	0.0821
C ₁₆₅	T _d	0.0000	T _d	0.0653
C ₃₂₃	T _d	0.0000	T _d	0.0183

3. Comparison of structure and stability

The results here indicate that the {100} nanodiamonds are the most stable of the structures tested, discounting the smallest cubic crystal. The dehydrogenated C₂₈ was found to be completely unstable, not surprisingly as the most stable structure for 28 carbon atoms is the C₂₈ fullerene. The remaining C₅₄ and C₂₅₉ {100} nanodiamonds retained the sp³ diamond structure following relaxation and exhibited (2×1) surface reconstructions and surface layer relaxations comparable to that of bulk diamond surfaces. This cannot be said for the remaining octahedral and cuboctahedral crystal structures.

Traditionally, the stability of nanodiamonds has been based on changes in bonding from sp³ to sp², which is determined here by the bond lengths. The sp³ bond length (characteristic of diamond) is 1.54 Å, whereas the graphite π bond length is 1.42 Å [31]. Therefore, a change in the C–C bond length from the sp³ length of ~1.54 Å, to ~1.42 Å length of sp² carbon, for a three-fold coordinated surface atoms is sufficient to identify a change of crystalline phase. It may therefore be seen by examination of the results obtained for the (111) surfaces of the octahedral and cuboctahedral crystals described above, that a phase transition to sp² carbon has occurred.

It is also possible to consider the stability of nanodiamond crystals in terms of changes in the symmetry; or more precisely, in terms of changes in the point group of the cluster. Bulk diamond is characterized by the T_d point group, as are cleaved diamond fragments such as the unrelaxed nanodiamonds. A change in the point group of the crystal upon relaxation, or a departure from the T_d point group outside an allowable tolerance may also be considered as indications of instability.

For each of the nanodiamond structures treated here, the point group has been determined using the program SYMMOL [32], which is based conceptually on the work of Pilati and Forni [33]. In this procedure, the quality of fit of an ideal point group to the actual structure is calculated. The results are contained in Table 2, for unrelaxed and relaxed structures. Listed is the point group of best fit and the error. Obviously, a large

error indicates a poor fit to the ideal point group, although, the point group may still be the most appropriate to the structure. Table 2 shows that each crystal with (111) surfaces, initially with the T_d bulk diamond point group, shows deterioration of point group symmetry upon relaxation; with the C₂₉ cuboctahedral and C₈₄ octahedral nanodiamonds changing from the T_d to the trigonal C_{3v} point group.

It was previously mentioned that the smallest cuboctahedral nanodiamond transformed into the endo-fullerene C–C₂₈. The C–C₂₈ complex was investigated with ab initio methods by Jackson et al. [34] in 1993. The findings reveal that the cage-atom interaction is a charge transfer from the endohedral atom to the cage, resulting in weak ionic bonding.

It is apparent from these results and the related experiments mentioned herein, that the surfaces of octahedral nanocrystalline diamond undergo a phase transition to the sp² structure. The separation of the outer sp² bonded shells of these new structures and the inner core of sp³ carbon was found to be approximately 2.25 Å. This is beyond the dissociation distance for the C–C covalent bond, and is shorter than the typical distance of 3.35 Å for the van der Waals bonds between the graphene sheets in crystalline graphite and carbon-onions. It is suggested then that a charge transfer resulting in weak ionic bonding is also responsible for the shell-core interaction in relaxed octahedral nanodiamonds.

4. Conclusion

It has been shown here that the results of our ab initio VASP study are in full agreement with previous experimental and theoretical findings. The results herein were found to show preferential graphitization and exfoliation of the (111) surfaces, both in octahedral and cuboctahedral morphologies, for nanodiamonds with the size range up to 1 nm in diameter. Hence, we conclude that dehydrogenated octahedral and cuboctahedral nanodiamonds represent unstable morphologies in this size range. Future plans include a Quantum Monte Carlo (QMC) relaxation of both dehydrogenated and hydrogenated nanodiamond, in search of both metastable and globally stable relaxation products. In addition to the continuing study of the structures described and mentioned here, further investigations are being undertaken on larger nanodiamonds, effects of hydrogenation, doping and a rigorous characterization of the properties of nanodiamond structures.

Acknowledgments

We would like to thank the Victorian Partnership for Advanced Computing and the Australian Partnership for

Advanced Computing supercomputer centre for their ongoing assistance over the course of this project.

References

- [1] J. Amlöf, H.P. Lüthi, *Supercomputer Research in Chemistry and Chemical Engineering*, ACS Symposium, ASC, W.A. 1987.
- [2] J.D. Johnson, M.S. Shaw, *Shock Compression of Condensed Matter – 1991*, Elsevier, Amsterdam, 1992, p. 333.
- [3] M.S. Shaw, J.D. Johnson, *J. Appl. Phys.* 62 (1997) 2080.
- [4] V.L. Kuznetsov, A.L. Chuvilin, Y.V. Butenko, I.Y. Mal'Kov, V.M. Titov, *Chem. Phys. Lett.* 209 (1994) 72.
- [5] V.L. Kuznetsov, I.L. Zilberberg, Y.V. Butenko, A.L. Chuvilin, B. Seagall, *J. Appl. Phys.* 86 (2) (1999) 863.
- [6] S. Tomita, T. Sakurai, H. Ohta, M. Fujii, S. Hayashi, *J. Chem. Phys.* 114 (17) (2001) 7477.
- [7] F.H. Ree, N.W. Winter, J.N. Glosli, J.A. Viecelli, *Phys. B* 265 (1999) 223.
- [8] N.W. Winter, F.H. Ree, *J. Comp. Aided Mater. Des.* 5 (1998) 279.
- [9] F. Fugaciu, H. Hermann, G. Seifert, *Phys. Rev. B* 60 (15) (1999) 10711–10714.
- [10] H. Hermann, F. Fugaciu, G. Seifert, *Appl. Phys. Lett.* 79 (1) (2001) 63–65.
- [11] A.S. Barnard, S.P. Russo, I.K. Snook, *Phil. Mag. Lett.* (2002) (accepted).
- [12] S.P. Russo, A.S. Barnard, I.K. Snook, *Surf. Rev. Lett.* (2002) (accepted).
- [13] F. Banhart, P.M. Ajayan, *Nature* 382 (1996) 433–435.
- [14] F. Banhart, *J. Appl. Phys.* 81 (8) (1997) 3440.
- [15] M. Zaiser, F. Banhart, *Phys. Rev. Lett.* 79 (1997) 3680–3683.
- [16] Ph. Redlich, F. Banhart, Y. Lyutovich, P.M. Ajayan, *Carbon* 36 (5–6) (1998) 561–563.
- [17] M. Zaiser, Y. Lyutovich, F. Banhart, *Phys. Rev. B* 62 (2000) 3058–3064.
- [18] R. Astala, M. Kaukonen, G. Jungnickel, Th. Frauenheim, R.M. Nieminen, *Phys. Rev. B* 63 (2001) 81 402.
- [19] G. Kresse, J. Hafner, *Phys. Rev. B* 47 (1993) RC558.
- [20] G. Kresse, J. Hafner, *Phys. Rev. B* 54 (1996) 11 169.
- [21] D. Vanderbilt, *Phys. Rev. B* 41 (1990) 7892.
- [22] G. Kresse, J. Hafner, *J. Phys.: Condens. Matter.* 6 (1994) 8245.
- [23] J. Furthmüller, J. Hafner, G. Kresse, *Phys. Rev. B* 50 (1994) 15 506.
- [24] G. Kern, J. Hafner, G. Kresse, *Surf. Sci.* 366 (1996) 445–463.
- [25] J. Perdew, Y. Wang, *Phys. Rev. B* 45 (1992) 13 244.
- [26] G. Kresse, J. Furthmüller, *Comp. Mat. Sci.* 6 (1996) 15.
- [27] D.M. Wood, A. Zunger, *J. Phys. A* 18 (1985) 1343.
- [28] A.S. Barnard, S.P. Russo, I.K. Snook, *Phil. Mag. B* 82 (17) (2002) 1767–1776.
- [29] Th. Frauenheim, U. Stephen, P. Blaudeck, D. Porezag, H.-G. Busmann, W. Zimmermann-Edling, et al., *Phys. Rev. B* 48 (24) (1993) 18189.
- [30] S.H. Yang, D.A. Drabold, J.B. Adams, *Phys. Rev. B* 48 (8) (1993) 5261.
- [31] R.C. Weast (Ed.), *CRC Handbook of Chemistry and Physics*, 65th ed, CRC Press, Inc, Boca Raton, 1984–1985.
- [32] T. Pilati, A. Forni, *J. Appl. Cryst.* 33 (2000) 417.
- [33] T. Pilati, A. Forni, *J. Appl. Cryst.* 31 (1998) 503.
- [34] K. Jackson, E. Kaxiras, M.R. Pederson, *Phys. Rev. Lett.* 48 (23) (1993) 17556–17561.